Hindawi
Journal of Nanomaterials
Volume 2022, Article ID 9221720, 12 pages
https://doi.org/10.1155/2022/9221720

Research Article

Analysis of Variable Compression Ratio Engine Using Biodiesel when Incorporated with Metal Oxides from Chemical and Biological Resources

M. Anish,[1] **T. Arunkumar**,[2] **J. Jayaprabakar**,[1] **T. Nivin Joy**,[1] **Sami Al Obaid**,[3] **Saleh Alfarraj**,[4] **M. M. Raj**,[5] **and Mebratu Markos**[6]

[1]*School of Mechanical Engineering, Sathyabama Institute of Science and Technology, Chennai, 600119 Tamilnadu, India*
[2]*Department of Mechanical Engineering, CMR Institute of Technology, Bengaluru, 560037 Karnataka, India*
[3]*Department of Botany and Microbiology, College of Science, King Saud University, PO Box -2455, Riyadh -11451, Saudi Arabia*
[4]*Zoology Department, College of Science, King Saud University, Riyadh 11451, Saudi Arabia*
[5]*Department of Mechatronics Engineering, Seoul National University of Science and Technology, Seoul 01811, Republic of Korea*
[6]*Department of Mechanical Engineering, College of Engineering, Wolaita Sodo University, Ethiopia*

Correspondence should be addressed to Mebratu Markos; mebratumarkos@wsu.edu.et

Received 6 March 2022; Accepted 3 May 2022; Published 30 June 2022

Academic Editor: Palanivel Velmurugan

Specifically, the current investigation will look at the impacts of nanoemulsions such as titanium and zinc oxides as well as plant extracts and a four-stroke D.I.VCR engine for biodiesel that is produced both chemically and biologically on the environment. Meanwhile, when a homogeneous catalyst is used, a substantial volume of wastewater is made available for the separation and cleaning of the biodiesel catalyst. Because of this, waste cooking oil (WCO) was used to make biodiesel, which were then transesterified using heterogeneous base catalysts. This was done for environmental reasons as well as to minimize the cost of producing biodiesel. The D.I variable compression engine's performance and engine parameters, such as brake specific fuel consumption, brake thermal efficiency, and CO, HC, and NOx emissions, were investigated. Nanoparticles have been shown to produce less NOx than pure diesel when combined with zinc oxides that have been biologically generated at the lowest possible concentration. The carbon dioxide emissions from a biologically generated titanium oxide sample are greater than those from the other samples, with Pure Diesel emitting the least amount of CO2. The emission of less oxygen from a Pure Diesel sample and a chemically generated titanium oxide sample showed a pattern that was comparable. A comprehensive study was conducted to examine the performance and emission characteristics of an internal combustion engine with and without the use of nanoadditives, and the findings revealed an astonishing outcome.

1. Introduction

Biodiesel vegetable oil is one of the renewable fuels that can be used in diesel engines with or without minor modifications. The use of biodiesel increases the oxygen content and increases combustion. Many of the characteristics of biodiesel are also identical to diesel. Nanoparticles have now been widely available for many products, including paints, lacquers, catalysts, biomedicine, cosmetics, skin creams, toothpastes, and many other applications, due to the rapid rise in nanotechnology over the last decade. The use of nanoparticle is suitable for the manufacturing industry due to its special physicochemical properties (e.g., magnetic, optic, and electrical features). Nanoparticles such as zinc oxides and titanium dioxide have been widely used in many fields in recent years. ZnO and TiO_2 nanoparticles were added as fuel catalysts in order to reduce the delay in ignition. The delay was decreased with a specific fuel consumption. In the form of nanopowder, the addition of metal and metal oxide to the base fuel may increase the propensity of the fuel. The interesting characteristics of nanoparticles are higher specific surface area, thermal conductivity,

catalytic activity, and chemical properties compared to their bulk shape. Nanoparticles have been used as biodiesel and diesel additives as new alternative fuel blends by a number of researchers. The use of fuel-borne catalysts benefits from improved fuel efficiency and unsafe greens. However, the consistency of the liquid fuels with the metal additives was a major problem, as the metal particles were easily settled. Increase the surface-to-volume ratio, allowing a rapid oxidation process with the incorporation of nanoparticles into fuel. Since the inventor Rudolph Diesel first tested peanut oil in his compression ignition engine, vegetable oils have been used as alternative fuels for 100 years. Today, it may seem insignificant that vegetable oils are used for motor fuels. However, these oils may be as essential over time as today's oil and coal tar products, but these nonconventional fuels have never been removed due to cheap oil products. Oils play an important role in the development of alternative fuels, although their use in diesel engines (especially direct injection engines) has posed a number of challenges. The main issue in the use of vegetable oils and animal fats is the high viscosity (approximately 11–17 times higher than diesel fuel) and the lower volatility that causes incomplete combustion of engine deposition due to incorrect vaporisation. Al_2O_3 Nanoparticles have been detected during oxygen reactions. Al_2O_3 is unstable during combustion at high temperatures, added methyl ester to nanoadditives improves combustion, improves engine performance and fuel suspension stability under CRDI, and adds Al_2O_3 to MME20D80 biodiesel ppm to minimize SFC by up to 7.66 percent. With the introduction of the MME20D80, fuel consumption will be increased by Al_2O_3 (100 ppm) compared with other biodiesels [1]. From the experiments, he found that with 100 ppm Al_2O_3 added to a maximum of 26.04 percent of HC emissions, the CO emissions are reduced when the engine is at a minimum load, but the CO emissions will be slightly higher at full load. Added Al_2O_3(50 ppm), the MME20D80 reduces by 26% of CO emissions but by 4.8% of NO_x, added with 100 ppm the MME20D80 reduces by 48% with the addition of Al_2O_3 (100 ppm) [2]. Ag nanoparticle with the size of 50 nm added with biodiesel reduces the SFC and increases the BTE to 5.58 percent, and the SFC decreases to 15 percent of the BSFC, and Ag also increases the engine power and the output torque with the addition of Ag as an additive [3]. Variable speed tests were carried out on a single cylindrical direct injection diesel engine using different biodiesel blends produced from waste vegetable oil. The analysis between the biodiesel blends and the diesel process has been carried out in terms of engine output and exhaust emissions. The engine worked smoothly without major problems with biodiesel mixtures. It has been noticed. Blends are more efficient with increased fuel efficiency and reduced emissions [4]. The CuO (50 ppm) added with MME20D80 reduces CO emissions for part load to 0.05%, reduces CO emissions by up to 0.23% for full load, and reduces emissions by HC-5.33%, CO-33%, and smoke-12.5% in total [5]. The addition of CeO_2 (90 ppm) to biodiesel with 5% of the H_2O emulsified at the highest load reduces NOx emissions but increases CO emissions due to the lack of oxygen [6]. The experiment would increase the BTE, reduce the temperature of the cylinder, reduce the friction in engines, raise the BSFC marginally, and improve overall combustion characteristics by the CeO_2 (90 ppm), used with the biodiesel by 5 percent emulsified H_2O [7]. The tests of the single-cylinder direct injection engine tests were carried out on diesels, jatropha oil, and oil mixtures in 97.4%, 2.6%, 80%, 20%, and 50% by volume. The test results have shown that jatropha oil can be effectively used in diesel engines as a diesel replacement [8].Even without engine modifications, it was satisfactory to run a test engine with pure coconut oil and coconut oil diesel blending for a wide range of engine conditions. The increase in coconut oil in coconut oil diesel fusion resulted in lower emissions of smoke and NO_x and an increase in fuel consumption due to the brakes [9]. Experiments with a single diesel engine cylinder using prey oil, soya oil, and its methyl esters as fuel. They have shown that esters and diesel-vegetable oil mixtures are close to diesel engine efficiency. Thanks to their low viscosity and low smoke production, methyl esters are suitable for longer use [10]. Torque and brake power were reported to be 3-5% lower than diesel fuel with the use of biodiesel-derived cooking oil. At increased engine rpm, the engine exhaust temperature was lower than that of diesel fuel [11].The addition of diesel-biodiesel to CNT has been shown to boost production efficiency by 3.67%, and the reduction of BTE by 5.57% is a small amount of specific fuel consumption. It is estimated that CNT will increase the number of octans and that CNT will be reactive to a large number of chemicals. CNT combined with vegetable ester made from the base fuel cooking oil can produce high temperatures and increase engine strength and output torque [12]. The introduction of diesel-biodiesel to CNT has been shown to improve output performance by 3.67%, and a small amount of specific fuel consumption is the reduction of BTE by 5.57%. CNT is calculated to increase the number of octans and to be reactive to a wide variety of chemical substances. CNT can produce a high temperature in combination with vegetable ester and increase engine strength and torque power output from base fuel cooking oil [13]. The experiment was conducted on the properties of the compression ignition engine and the use of mixtures of jatropha oil and diesel fuel. Due to the reduced viscosity of the type of diesel vegetable oil, the exhaust gas temperature has been reduced. It was found that a higher proportion of jatropha oil was used in mixtures to increase fuel consumption. Including blends of up to 50% (by volume) of jatropha oil, acceptable thermal efficiency of the engine was achieved. [14, 15]. Added to D40B30E30 with ZnO (250 ppm), CO emissions will be reduced but higher at minimum HC emissions. Full combustion occurs at full load, thus reducing emissions of HC. It has higher CVs so that NO_x emissions are increased, but it reduces smoke emissions [16]. Biodiesel ethanol fuel fuses with the addition of ZnO at 250 ppm at different temperatures. Added mixtures of ZNO metal oxide to the fuel will increase the fuel CV and the BSFC rate, the heat release rate, and the cylinder pressure, but the total load will increase with BTE, and experimentally, it was found that the addition of ZNO palm oil at 225 ppm would improve the BTE and increase the EGT at high load [17, 18]. Presented

Table 1: Properties of ZnO and TiO_2.

Parameter	Units	Zinc oxide	Titanium dioxide
Molecular weight	g/mole	81.40	79.87
Energy gap	eV	3.37	3.2
Exciton energy	meV	60	—
Density	g/cm^3	5.606	3.895
Lattice constants	nm	$A = 0.3296$, $c = 0.52065$	$A = 0.3758$, $c = 0.9514$
Boiling point	K	2633.15	3245
Melting point	K	2248.15	2116
Refractive index	nD	2.0041	2.488
Thermal conductivity, K	W/mK	50	11.7
Thermal expansion, α	10^{-6} K^{-1}	4.31	9

the results of the engine test with different blends, clean rapeseed oil, and diesel fuel. There were no significant problems with the operation of the engine using these alternative fuels. Test results showed a reduction in brake thermal efficiency as the amount of rapeseed oil in the blend increased. Reduction of power output was also noted with an increase in emissions [19]. The CNT, combined with diesel-diesel, reduces CO and Soot emissions and increases NO_x emissions. CNT (5 nm) biodiesel results in an increase in hC emissions and a reduction in CO emissions. CO_2 and NO_x emissions are reduced by CO and HC emissions [20]. The addition of CuO (50 ppm) to the MME20D80 reduces SFC and improves heat quality, 1.3 percent BTE increases at full load, BTE decreases, and the percentage of blends is higher. The introduction of FBC in biodiesel has a significant impact on braking strength, SFC, and emission efficiency due to increased cylinder gas pressure and reduced ignition time under optimized operating conditions [21]. Metal additives can effectively minimize emissions by either combining them with water to produce hydroxyl radicals that increase soot oxidation or by reacting directly to soot carbon atoms and thus lowering the oxidation temperature. However, the application of FBC to biodiesel showed a small increase in NO and CO_2 emissions under optimized operating conditions [22]. According to the summary of the above literature review, numerous researchers used various types of nanoadditives with varying dimensions, and some researchers worked with nanoadditives at varied operating temperatures, according to the summary. No additional research has been done on nanoadditives in combination with chemical and biological systems as a consequence of this fact. This will be the first time that chemical and biological nanofluids will be used in studies of this kind. This research will examine the effects of nanoemulsions for biodiesel that is chemically and biologically generated, such as oxides of titanium and zinc, plant extract, and four-stroke D.I.VCR engine. In the meantime, a great deal of wastewater is available using a homogenous catalyst to isolate and purify the catalyst from biodiesel. Biodiesel has therefore been produced from a waste cooking oil (WCO), transesterified with heterogeneous base catalysts, for environmental reasons and to reduce production costs for biodiesel. Biodiesel has been developed using heterogeneous base catalysts in waste cooking oil (WCO). The D.I variable compression engine evaluated output and engine features such as basic fuel consumption braking, thermal brake efficiency, CO, HC, and NO_x emissions.

Table 2: Biodiesel properties.

Density	0.880 g/cc
Kinematic viscosity @ 40°C	1.54 cSt
Flash point	188°C
Fire point	202°C
Moisture content	0.31%
Calorific value	6912.82 Cal/g

2. Materials and Methods

2.1. Chemical Synthesis of Zinc Oxide Nanoparticles. Zinc acetate is the initial material used in this process. Originally, 1 m zinc acetate was intelligently agitated, and 2 M caustic soda was wisely applied to the new cleverly agitated zinc acetate. Instead, there was a lot of white slurry, and the white precipitate suspension was constantly stirred for eighteen hours. Filtered and washed with water in a muffle chamber and ground to fine powder and calcined at 400°C. If the temperature is above 400°C, the particles degrade and the color changes are observed between the colors in white and dark ash.

2.2. Biological Synthesis of Zinc Oxide Nanoparticles. Nanoparticles are prepared in this method from extracts of the Hibiscus Rosa-Sinensis leaf. Leaf extract of approximately 50 ml was taken and boiled using a stirrer at 70°C. The solution was applied with 5 grams of zinc nitrate, as the temperature exceeds 70°C. Boiling occurs before a yellow-colored paste enters the mixture. For collecting the paste, a ceramic crucible was used and heated in a furnace for 2 hours at 400°C. It obtains a soft white color powder, which is collected and used for further purposes.

2.3. Chemical Synthesis of Titanium Dioxide Nanoparticles. This was based on titanium tetra chlorine (TiCl4). TICL4 50 ml of distilled water has been added to 200 ml of ice-cold water. The beaker is transported from ice-cooled space

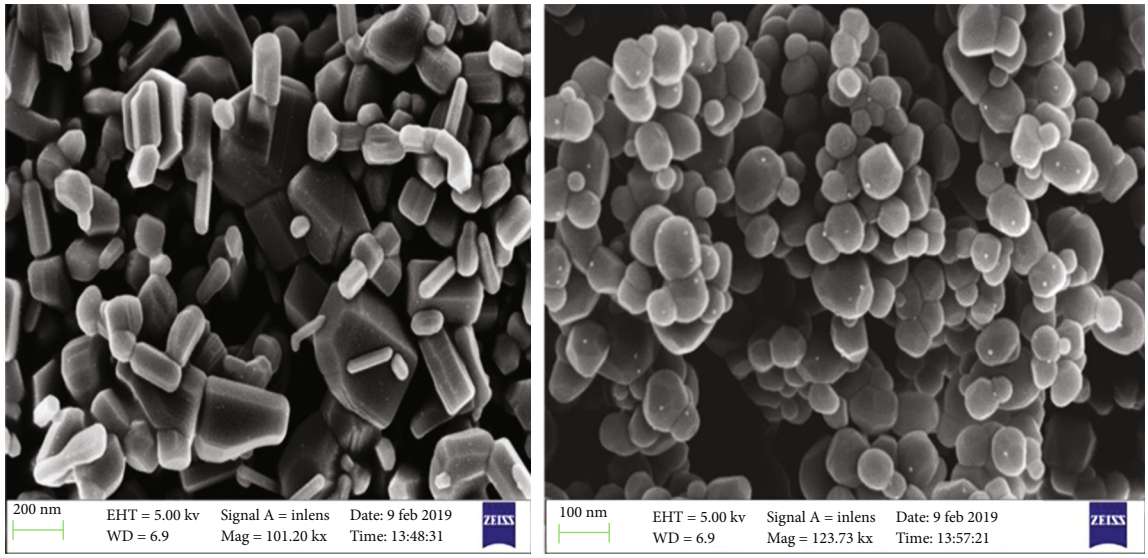

Figure 1: SEM image of chemically synthesized zinc oxide and titanium oxide nanoparticles.

to room temperature. The magnetic stirrer was pumped in a beaker for 30 minutes to produce a homogeneous solution. The temperature of the bath will rise to 150°C and will remain at the same temperature until the extraction of nanoparticulate matter is complete.

2.4. Biological Synthesis of Titanium Dioxide Nanoparticles. In this process, nanoparticles are produced from Moringa oleifera leaf extracts. The collected leaves are washed and dried for 7 days in sunlight. Then, the bits were cut and broken into powder. Take 10 grams of this powder with 100 ml of ethanol. The mixture is heated at 50°C for an hour. As a result, the mixture is cut to ethanolic leaf extract with Whatman filtering paper. This extract was reacted with 0.5 M of titanium tetraisopropoxide at 50°C. After 3 hours of mixing and 15 minutes of centipilation, 5000 rpm titanium dioxide nanoparticles were obtained.

Comparative properties for blending with biomass diesel for use in zinc oxide and titanium dioxide nanoparticles are evaluated in Table 1. In total, nanoparticles with these requirements may be used for the combination of efficiency and emission properties with biodiesel.

2.5. Preparation of Biodiesel. Biodiesel is prepared from the method of transesterification, which is the method of using an alcohol such as methanol, ethanol as a catalyst by using a caustic soda or potassium hydroxide. For a substance like glycerol, the catalyst chemically splits the raw oil molecules into methyl esters. The 1-liter palm oil is in a bowl and is heated with a heater to 70°C. The temperature then falls to 55°C. During this time, the mixer should be tested for dry and cleaning, and the components should be tightly installed. The 1 liter bottle contains methanol of 200 ml. The water is drained by methanol from the atmosphere and should be carried out rapidly. The lid of the container should be kept tight. The bottle is then filled with NaOH funnel and swirled around for some time. The reaction is heated by the mixture. Sodium methoxide is formed when NaOH is completely dissolved by methanol. In a blender, they take the heated oil. Sodium methoxide is carefully moved from the container to the liquid so that the blender is turned off. The blender is then turned on for 20 minutes while the lid is closed. The container is covered with a wet towel to prevent overheating. The mixture is taken to a 2-liter pet bottle after the process has been completed, and the lid is tightly closed. After 24 hours, the bottom of the bottle is filled with dark glycerine. It is separated from the pale fluid on top of which organic diesel is needed. Organic diesel is to be washed to remove soap, catalyst, and other impurities. Organic diesel is used for cleaning in a washing container with half a liter of fresh H_2O. The bottle is tightly fitted and rolls on the side before the oil and the H_2O are combined. The chemical properties obtained by biodiesel for use in diesel engines have been analyzed in Table 2. Overall, there have been no significant variations in density, kinematic viscosity compared to ASTM biodiesel standards, while flash and fire point are at a temperature higher than the ASTM standards. The biodiesel developed is therefore mixed with diesel, and the engine tests are performed with these characteristics.

2.6. SEM Analysis of Chemically Synthesized Zinc Oxide of Nanoparticle. Scanning electron microscopy (SEM) images of zinc oxide nanoparticles have been obtained using the ZEISS scanning electron microscope. It has a high 2 nm, 3 nm @ 30 kV resolution. SEM displays nanoparticle zinc oxide under ZEISS electron scanning microscopy. EHT refers to the high voltage electron which is the electrons' accelerating energy. From the picture, the particle size of nano is clearly visible in the range of nanometres. Zinc oxide nanoparticulates were collected with a ZEISS electron microscope scanning microscope (SEM). The resolution is high 2 nm. The SEM image shown in the ZEISS scanning electron microscope reveals nanoparticles of titanium dioxide. The particles are in the meter scale, as can be seen from the image above (Figure 1).

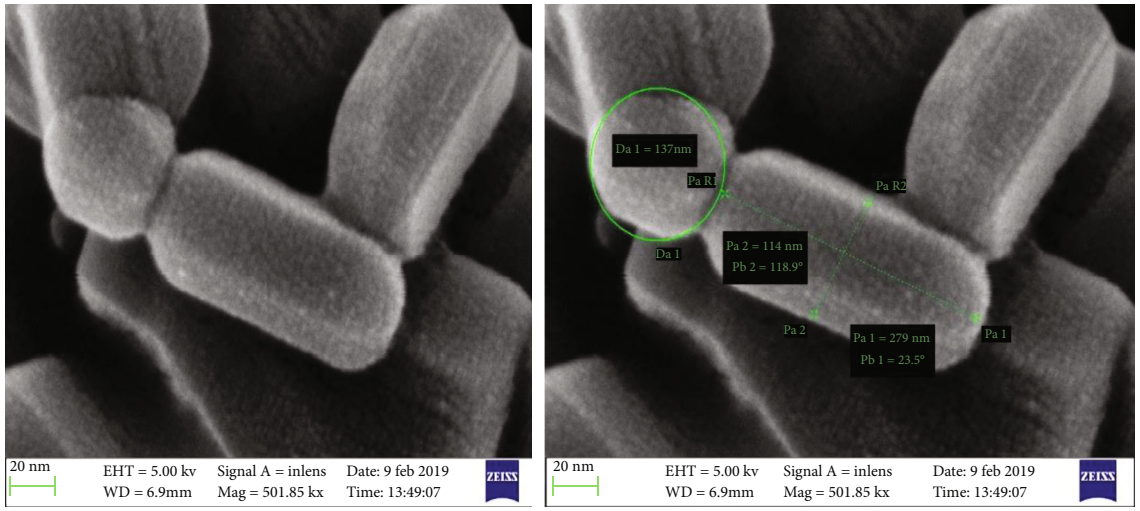

Figure 2: SEM image of biological synthesized zinc oxide nanoparticles.

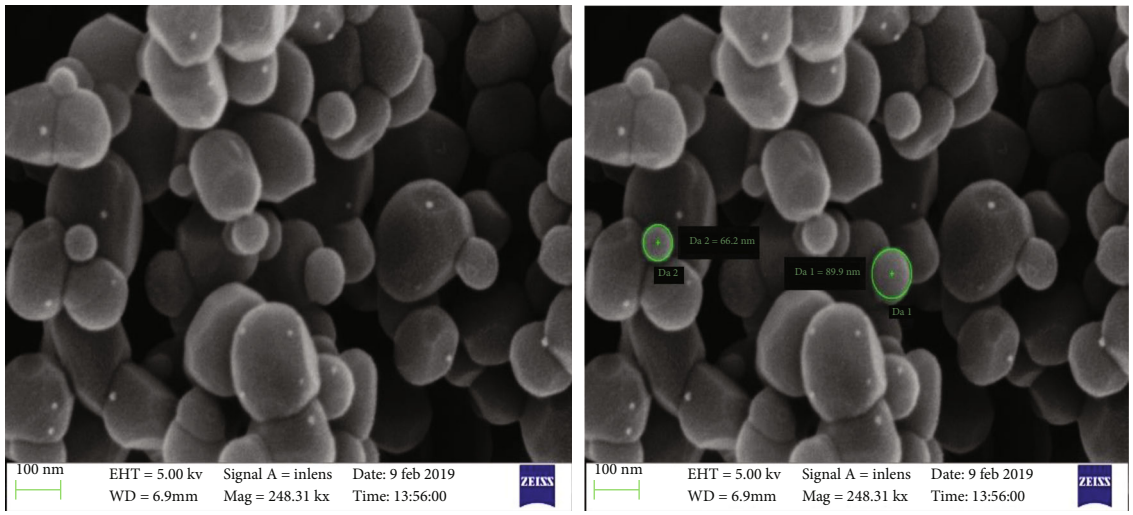

Figure 3: SEM image of biological synthesized titanium oxide nanoparticles.

2.7. SEM Analysis of Biological Synthesized Zinc and Titanium Oxide Nanoparticle. As the image in Figure 2 of the SEM clearly shows, the particles are in nanometer range, and the surface of the nanoparticles is a bit rough. The morphologies of the nanoparticles are changed based on the temperature of the calcination. The SEM image shows that the readings for this nanoparticle are taken as 5.9 mm as the working distance of 5 kV electron high voltage, i.e., the velocity of the electrons. The image shows the different sizes of nanoparticles, all of which are within the nanometer range. WD refers to the working distance, i.e., the distance between the lens and the sample. As shown in the image below, the nanoparticles are slightly coagulated with each other (Figure 3).

2.8. Preparation for Engine Testing. Nanoparticle preparation is combined with biodiesel. This means that 400 ml of diesel is blended into 100 ml of biodiesel, which means that 20 percent of the sample fuel is biodiesel and the remainder is petrol. A total of 4 such samples are available, combining a nanoparticle of 150 ppm per sample. Each sample is provided for engine and output, and emission characteristics can be observed. (The samples are short named as S1, S2, S3, and S4. S1—ZnO chemically synthesized, S2—TiO_2

Table 3: Engine specifications.

Engine type	4 stroke diesel, single cylinder
Bore × stroke	87 × 110 mm
Swept volume	661.45 cc
Compression ratio	18 : 1
Rated power	3.50 kW @ 1500 rpm
Cooling system	Water cooling

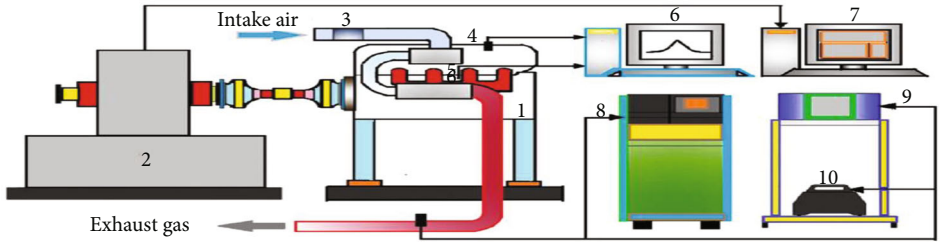

1. Test engine
2. Eddy current dynamometer
3. Air mass sensor
4. Pressure sensor
5. Accelerometer
6. Data aquisition system (DAS)
7. Dynamometer controller
8. Bosch gas analyser
9. AVL digas analyser
10. Smoke opacity meter

Figure 4: Engine test rig.

Table 4: Instruments used selection, precision, and percentage vulnerability.

Instrument	Measured quantity	Range	Accuracy	Uncertainties (%)
AVL Di-gas 444 analyzer	NO_x	0–5000 ppm	±10 ppm	±0.5%
	HC	0–20,000 ppm	±10 ppm	±0.1%
	CO	0–10% vol.	±0.03%	±0.3%
AVL 437C smoke meter	Smoke opacity	0–10 FSN	±1%	±1.0%
Speed sensor	Engine speed	0–10,000 rpm	±10 rpm	±0.1%
Burette	Fuel quantity	0–1000 cc	±0.1 cc	±1.0%

chemically synthesized, S3—TiO_2 biologically synthesized, S4—ZnO biologically synthesized).

From Table 3, the diesel engine having these specifications was primarily started with diesel and then with the produced test fuels. Speed of the engine was maintained constant speed at 1500 rpm under varying load conditions to measure the performance parameters such as brake thermal efficiency, specific fuel consumption (SFC), and exhaust gas temperature and also to measure the emission parameters like carbon monoxide (CO), unburnt hydrocarbon (HC), and nitrogen oxide (NO) emissions for both diesel and the prepared test fuels. The schematic diagram of the tested engine is depicted in Figure 4.

2.9. Accuracy and Uncertainties. Errors and uncertainties can result from various factors, such as instrument selection and calibration, changing environmental conditions, testing, observations, etc. Uncertainty can usually be divided into two key sources, set and spontaneous mistakes. In the previous example, repeatability is debated, and in the second, the analysis is treated [23–26]. In the confidence limits of ±2 ± Gaussian distribution, the uncertainty of measured variable (axis X) is assessed as shown in equating (1). 2σ is the average limit on which the calculated values fall on 95%.

$$\Delta X_i = \frac{2\sigma_i}{X_i} * 100, \tag{1}$$

where X_i is the readings figure and refers to experimental read and standard deviation. With the following

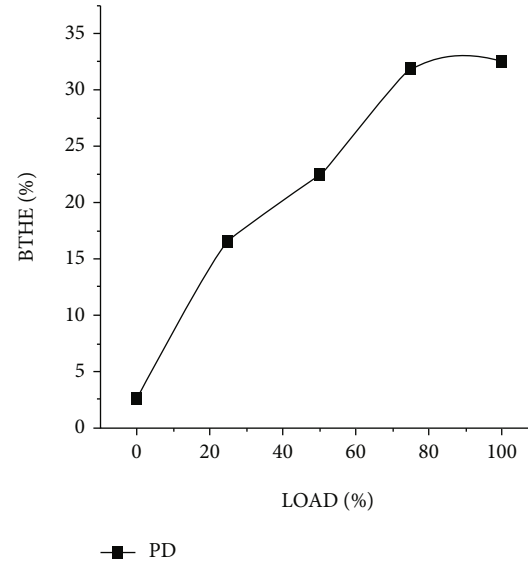

Figure 5: Load vs. brake thermal efficiency for pure diesel sample.

statement, the uncertainties of measured parameters were evaluated.

$$R = f(X1, X2, X3, \cdots \cdots \cdots \cdots ..Xn), \tag{2}$$

$$\Delta R = \sqrt{\left[\left(\frac{\partial R}{\partial X1}\Delta X1\right)^2 + \left(\frac{\partial R}{\partial X2}\Delta X2\right)^2 + \left(\frac{\partial R}{\partial X3}\Delta X3\right)^2 + .. \cdots \cdots \cdots \cdots \cdots \cdots \left(\frac{\partial R}{\partial Xn}\Delta Xn\right)^2\right]}, \tag{3}$$

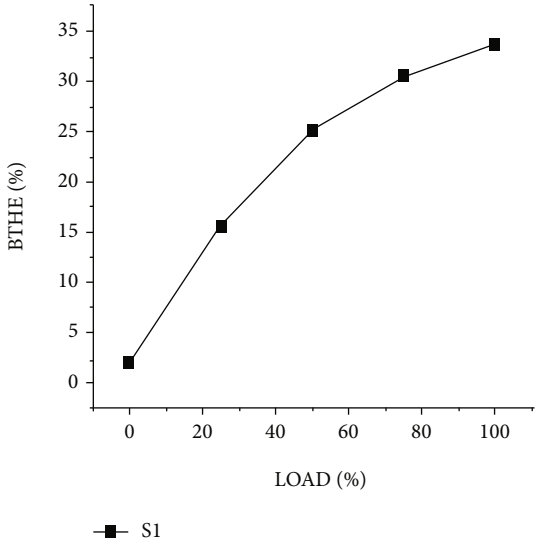

Figure 6: Load vs. brake thermal efficiency for S1 sample.

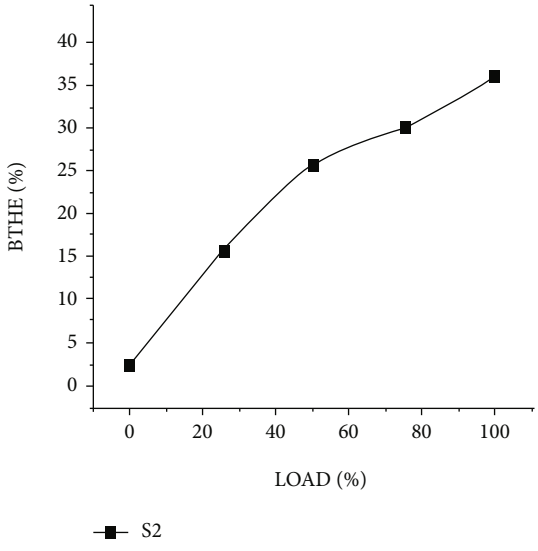

Figure 7: Load vs. brake thermal efficiency for S2 sample.

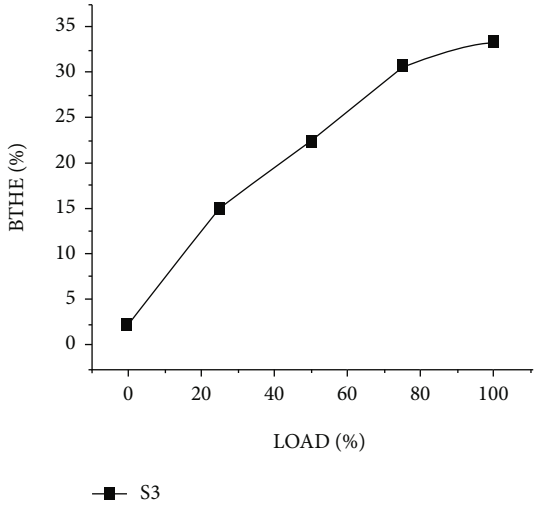

Figure 8: Load vs. brake thermal efficiency for S3 sample.

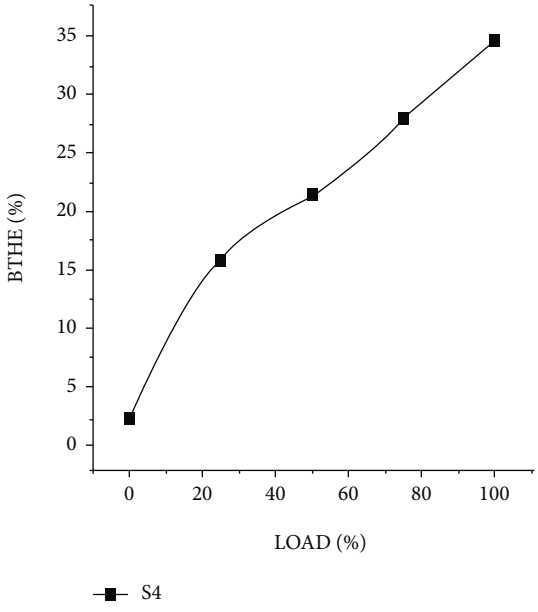

Figure 9: Load vs. brake thermal efficiency for S4 sample.

where "R" in Equation (2) represents the function of $X1$, $X2, \cdots \cdots ..Xn$, and $X1, X2, \cdots .Xn$ represents the number of readings taken. Hence "ΔR" is computed by RMS (root mean square) of errors associated with measured parameters. The uncertainties of various measuring instruments were illustrated in Table 4.

3. Results and Discussion

3.1. Performance Characteristics. The following graphs show the information on the thermal efficiency brake and the load for five different samples. It is clear from Figure 5 that pure diesel has an efficiency of about 32 percent at maximum load. Efficiency decreased slightly at 30% load and continued to increase at a later date. Figure 6 shows that the S1 sample has a continuous increase in efficiency without any deviation. Figure 7 shows that the efficiency decreases slightly at a load of 60 percent for the S2 sample. Figure 8 shows that the S3 sample has the same PD sample path as the efficiency decreases slightly at a load of 30 percent and increases continuously. Figure 9 shows load vs. brake thermal efficiency for S4 sample.

From Figure 10, each nanoparticle and pure diesel shows an increase in the percentage of brake thermal efficiency with an increase in load. All the samples almost gave a similar increase in the BTE percentage up to 30% of the load and started to vary. The S1 and S2 samples showed a constant increase, while the efficiency of the pure diesel and S3 samples decreased after 30% of the load. On the other hand, the S4 sample gave the least efficiency, and pure diesel showed an efficiency of 30 percent at 80 percent of the load, which is the highest percentage of BTE obtained by any

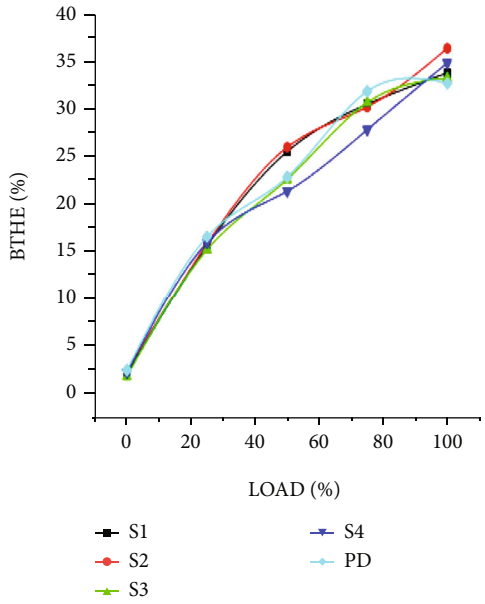

Figure 10: Load vs. brake thermal efficiency for five different samples.

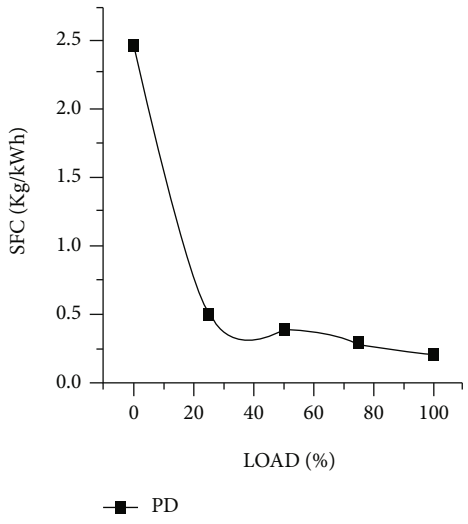

Figure 11: Load vs. SFC for PD sample.

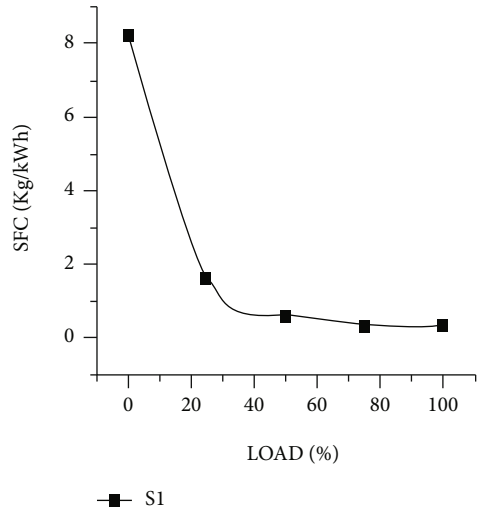

Figure 12: Load vs. SFC for S1 sample.

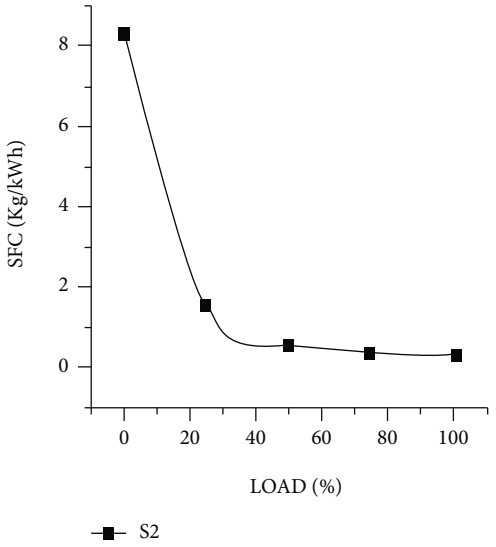

Figure 13: Load vs. SFC for S2 sample.

sample until then. All samples tend to show a similar BTE percentage at 100 percent load again. Overall, chemically prepared nanoparticle samples, i.e., S1 and S2 showed an impressive result when compared to other samples.

3.2. Specific Fuel Consumption. The following graphs illustrate the specific fuel consumption information for five different samples. From Figure 11, it is shown that pure diesel has an SFC of 2.5 kg/kWh at initial load which is quite low, and that the graph at maximum load is much lower. Figure 12 shows that the SFC is 8 kg/kWh at the beginning and has decreased since then. It is clear from Figure 13 that the graph suddenly decreases just like other graphs and is constant from then on. From Figure 14, the SFC is approximately 12 kg/kWh at the initial load, which is high at the start and then decreases. From Figure 15, the SFC is approximately 5 kg/kWh for the S4 sample and decreases slowly thereafter.

From Figure 16, all the samples showed a decrease in fuel flow rate with increase in load. S2 sample portrayed higher consumption of fuel of about 12 kg/kWh at the start, and the same sample showed the least fuel consumption at 40% load. Pure diesel depicted the least consumption of fuel and maintained a constant path from 20% load. S3 sample has the highest fuel consumption till 50% of load. On the other hand, the graph of S1 sample gradually kept falling till 50% and the same to S4 sample. All the samples have the same fuel consumption from 50% load. Overall, the samples with nanoparticles have higher fuel consumption than pure diesel. S1 and S2 samples have higher SFC in the start whereas S3 and S4 have higher SFC from 20% load.

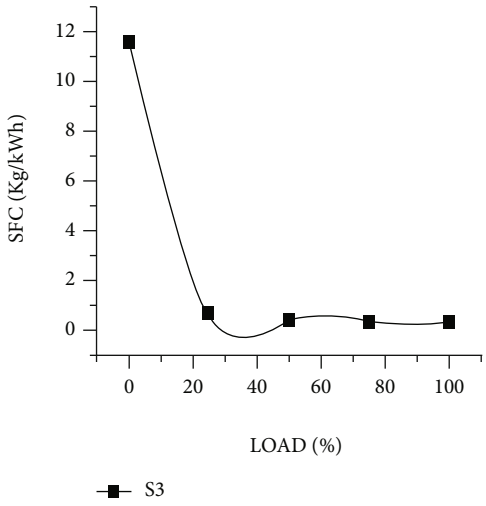

Figure 14: Load vs. SFC for S3 sample.

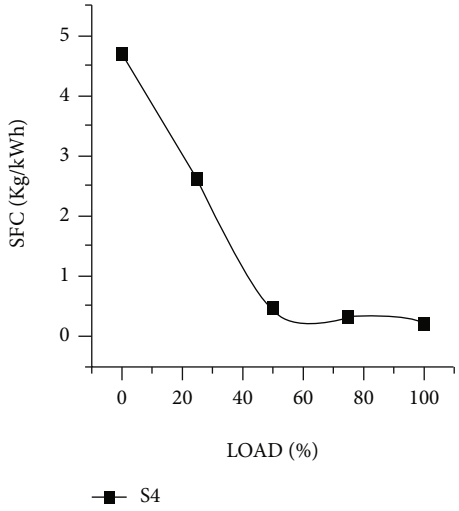

Figure 15: Load vs. SFC for S4 sample.

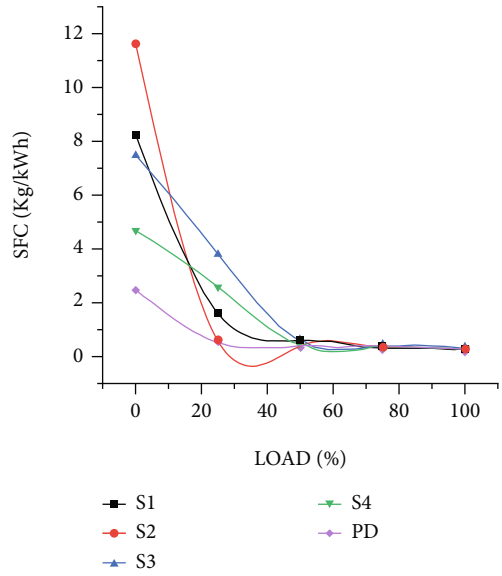

Figure 16: Load vs. SFC for five samples.

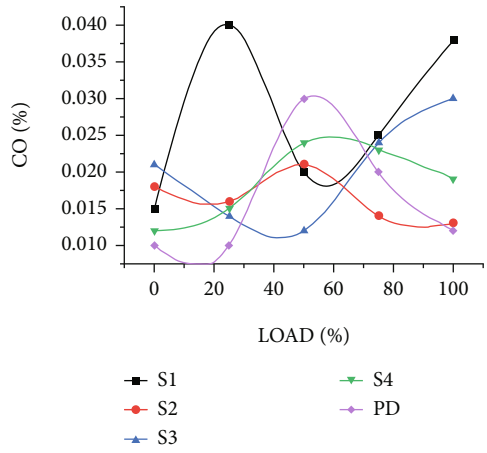

Figure 17: Load vs. carbon monoxide emission for five different samples.

3.3. Carbon Monoxide Emissions. The following graph obtained depicts the information about carbon monoxides and load for five different samples.

Pure diesel showed a constant increase and decrease in the percentage of carbon monoxide in Figure 17, just like the rest of the graphs. The S1 sample showed a high CO content release at the initial load, except that each sample showed a reduction in CO emissions of up to 25% of the load and then the CO percentage started to rise. From 50% load, these samples again showed a decrease in CO emissions, with S1 being the highest carbon monoxide emission at 100%. Overall, S1 has the highest CO emission content, while pure diesel has the lowest CO emission.

3.4. Hydrocarbon Emissions. The following graph obtained depicts the information about hydrocarbon emissions and load for five different samples. From Figure 18, the lines go fluctuating throughout the graph for every sample. S3 sample portrayed a sudden rise in HC emissions till 25% and started decreasing from then and similar path is followed by S3 sample. Pure diesel and S4 sample depicted an opposite trend in HC emissions. Overall, except S2 and PD, every sample showed a decrease in HC emission at maximum load.

3.5. Oxides of Nitrogen. The following graph obtained depicts the information about oxides of nitrogen emissions and load for five different samples.

From Figure 19, pure diesel has a stable increase in graph whereas for the rest, the graph goes fluctuating. There is a rise in the NOx emissions till 20% for all the samples. From then onwards, the graph decreases for S3 and S4 samples which depict the least NOx emission at 50%. The graph for S2 and S1 almost remained the same till 50% load at which

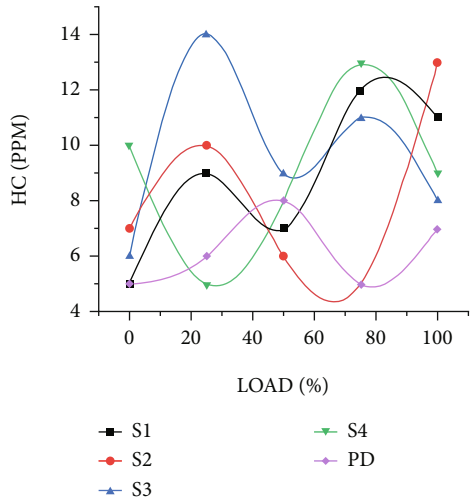

Figure 18: Load vs. hydrocarbon emission for five different samples.

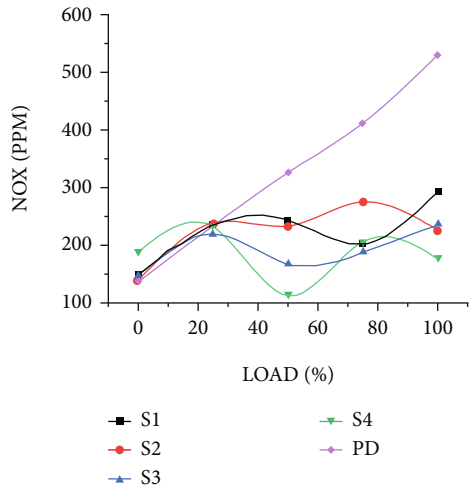

Figure 19: Load vs. oxides of nitrogen emission for five different samples.

they meet. Overall, the nanoparticle samples showed an impressive result in emitting less NOx than the pure diesel with S4 sample touching the least value.

3.6. Carbon Dioxide and Oxygen Emissions. Hydrocarbons (HC) react with oxygen (O_2) to produce water vapour and carbon dioxide.

From Figure 20, all the graphs depicted various trends in emission of CO_2. Pure diesel being the sample to have a sudden increase of 5 percent in emission from 50% load. S2 sample has constant increase whereas S4 and S2 showed a similar graph. Overall, the carbon dioxide emissions are higher for S3 than the rest of the samples with PD sample being the least emitter of CO_2.

From Figure 21, pure diesel, S2, portray the same trend whereas the samples S3 and S4 gave similar oxygen emissions. S1 sample gave fluctuating graph with increase in load. Overall, PD and S2 sample gave similar trend in emitting less oxygen emissions.

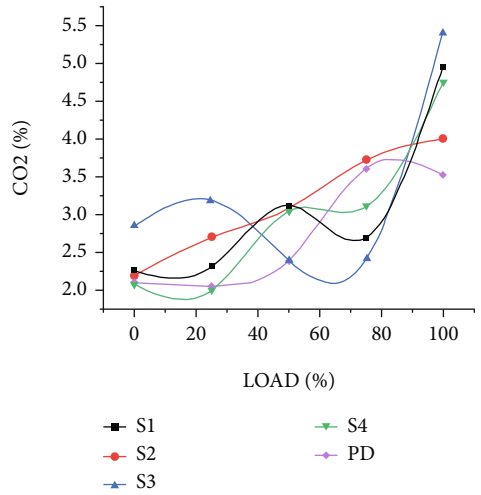

Figure 20: Load vs. carbon dioxide emission for five different samples.

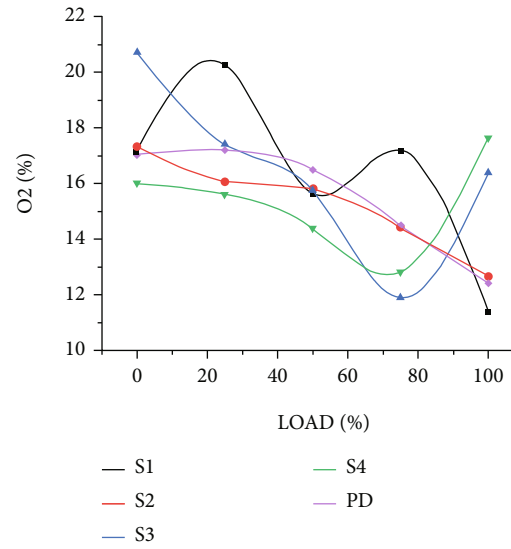

Figure 21: Load vs. oxygen emissions for five different samples.

4. Conclusion

The chemical samples of nanoparticles, as well as their performance properties, are described in detail. In comparison to prior investigations, S1 and S2 show significant improvements in brake thermal efficiency. For pure diesel, the fuel consumption of samples containing nanoparticles is greater than that of control samples, and in the beginning, S1 samples with higher SFC are more fuel efficient. S1 has the largest CO emission volume characteristic for emissions, whilst S2 has the lowest pure diesel emission volume characteristic for emissions. With the exception of the S2 sample and the PD, each sample demonstrated a decrease in maximum load HC emission. A stunning result was obtained from the nanoparticle samples, with just the tiniest amount of NOx emitted when S4 was used in pure diesel. In comparison to the other samples, carbon dioxide emissions from the S3 sample are much greater, with the PD sample emitting the

least amount of CO2. When it came to the emission of less oxygen, both the PD and S2 samples exhibited comparable tendencies. Overall, the performance and emission characteristics of the diesel engine are compared with and without the addition of nanoadditives, and the findings demonstrate that the inclusion of nanoadditives has a significant impact on both.

Abbreviations

WCO: Waste cooking oil
FFA: Free fatty acids
BTE: Brake thermal efficiency
BSFC: Brake specific fuel consumption
CO: Carbon monoxide
CO2: Carbon dioxide
HC: Hydrocarbon
NOx: Oxides of nitrogen
SFC: Specific fuel consumption
EGT: Exhaust gas temperature
CI: Compression ignition.

Data Availability

The authors confirm that the data supporting the findings of this study are available within the article. Further data or information is available from the corresponding author upon request.

Conflicts of Interest

The authors declare that there are no conflicts of interest regarding the publication of this paper.

Acknowledgments

The authors appreciate the support from Wolaita Sodo University, Ethiopia. The authors thank Sathyabama Institute of Science and Technology and CMR Institute of Technology for providing assistance to complete this work. This project was supported by Researchers Supporting Project number (RSP-2021/315) King Saud University, Riyadh, Saudi Arabia.

References

[1] A. Gog, M. Roman, M. Toşa, C. Paizs, and F. D. Irimie, "Biodiesel production using enzymatic transesterification - current state and perspectives," *Renewable Energy*, vol. 39, no. 1, pp. 10–16, 2012.

[2] A. Kołodziejczak-Radzimska and T. Jesionowski, "Zinc oxide—from synthesis to application: a review," *Materials*, vol. 7, no. 4, pp. 2833–2881, 2014.

[3] G. Antolin, V. F. Tinaut, Y. Briceno, V. Castano, C. Perez, and A. I. Ramırez, "Optimisation of biodiesel production by sunflower oil transesterification," *Biotech*, vol. 83, pp. 111–114, 2002.

[4] I. M. Atadashi, M. K. Aroua, A. R. Abdul Aziz, and N. M. N. Sulaiman, "Production of biodiesel using high free fatty acid feedstocks," *Renewable and Sustainable Energy Reviews*, vol. 16, no. 5, pp. 3275–3285, 2012.

[5] S. H. Cha, J. Hong, M. Mcguffie, B. Yeom, J. S. Vanepps, and N. A. Kotov, "Shape-dependent biomimetic inhibition of enzyme by nanoparticles and their antibacterial activity," *ACS Nano*, vol. 9, no. 9, pp. 9097–9105, 2015.

[6] X. Chen and S. S. Mao, "Titanium dioxide nanomaterials: - synthesis, properties, modifications, and applications," *Chemical Reviews*, vol. 107, no. 7, pp. 2891–2959, 2007.

[7] R. C. Frank, P. Luc, and W. Arnaldo, *A global overview of vegetable oils, with reference tobiodiesel*, vol. 9, no. 19, 2009, IEA,Bioenergy, London, 2009.

[8] R. Hong, T. Pan, J. Qian, and H. Li, "Synthesis and surface modification of ZnO nanoparticles," *Chemical Engineering Journal*, vol. 119, no. 2-3, pp. 71–81, 2006.

[9] G. Huang, F. Chen, D. Wei, X. W. Zhang, and G. Chen, "Biodiesel production by microalgal biotechnology," *Applied Energy*, vol. 87, no. 1, pp. 38–46, 2010.

[10] Y. Lan, Y. Lu, and Z. Ren, "Mini review on photocatalysis of titanium dioxide nanoparticles and their solar applications," *Nano Energy*, vol. 2, no. 5, pp. 1031–1045, 2013.

[11] Y. Li, W. Zhang, J. Niu, and Y. Chen, "Mechanism of photogenerated reactive oxygen species and correlation with the antibacterial properties of engineered metal-oxide nanoparticles," *ACS Nano*, vol. 6, no. 6, pp. 5164–5173, 2012.

[12] K. Malachová, P. Praus, Z. Rybková, and O. Kozák, "Antibacterial and antifungal activities of silver, copper and zinc montmorillonites," *Applied Clay Science*, vol. 53, no. 4, pp. 642–645, 2011.

[13] T. Martinez, A. Bertron, E. Ringot, and G. Escadeillas, "Degradation of NO using photocatalytic coatings applied to different substrates," *Building Environment*, vol. 46, no. 9, pp. 1808–1816, 2011.

[14] H. Park, H. I. Kim, G. H. Moon, and W. Choi, "Photoinduced charge transfer processes in solar photocatalysis based on modified TiO_2," *Energy Environmental Science*, vol. 9, no. 2, pp. 411–433, 2016.

[15] L. E. Rincon, J. J. Jaramilo, and C. A. Cardona, "Comparison of feedstocks and technologies for biodiesel production: an environmental and techno-economic evaluation," *Renewable Energy*, vol. 69, pp. 479–487, 2014.

[16] Y. C. Sharma and B. Singh, "Development of biodiesel: current scenario," *Renewable and Sustainable Energy Reviews*, vol. 13, no. 1646, p. 51, 2009.

[17] M. Canakci and J. Van Gerpen, "Biodiesel production from oils and fats with high free fatty acids," *Transactions of the ASAE*, vol. 44, no. 6, pp. 1429–1436, 2001.

[18] J. M. Marchetti, V. U. Miguel, and A. F. Errazu, "Techno-economic study of different alternatives for biodiesel production," *Fuel Processing Technology*, vol. 89, no. 8, pp. 740–748, 2008.

[19] P. Tschakert, E. Huber-Sannwald, D. S. Ojima, M. R. Raupach, and E. Schienke, "Holistic, adaptive management of the terrestrial carbon cycle at local and regional scales," *Global Environmental Change*, vol. 18, no. 1, pp. 128–141, 2008.

[20] G. Chen, M. Ying, and W. Li, "Enzymatic conversion of waste cooking oils into alternative fuel-biodiesel," *Applied Biochemistry and Biotechnology*, vol. 129, pp. 911–921, 2006.

[21] M. M. R. Talukder, P. Das, T. S. Fang, and J. C. Wu, "Enhanced enzymatic transesterification of palm oil to biodiesel," *Biochemical Engineering Journal*, vol. 55, no. 2, pp. 119–122, 2011.

[22] A. Murugesan, C. Umarani, R. Subramanian, and N. Nedunchezhian, "Bio-diesel as an alternative fuel for diesel engines–a review," *Renewable and sustainable energy reviews*, vol. 13, no. 3, pp. 653–662, 2009.

[23] M. Vinayagam, S. S. Kumar, M. M. Ravikumar, S. Mahendiran, and T. Raja, "Feasibility and emission study on employing MgO nanoparticle as oxygenated additive in neat biodiesel," *International Journal of Ambient Energy*, vol. 42, no. 14, pp. 1629–1634, 2021.

[24] P. Appavu, J. Jayaraman, and H. Venu, "NOx emission reduction techniques in biodiesel-fuelled CI engine: a review," *Australian Journal of Mechanical Engineering*, vol. 2022, pp. 1–11, 2019.

[25] C. C. Akoh, S. W. Chang, G. C. Lee, and J. F. Shaw, "Enzymatic approach to biodiesel production," *Journal of Agricultural and Food Chemistry*, vol. 55, no. 22, pp. 8995–9005, 2007.

[26] C. Y. Lin and C. Lu, "Development perspectives of promising lignocellulose feedstocks for production of advanced generation biofuels: a review," *Renewable and Sustainable Energy Reviews*, vol. 136, article 110445, 2021.